

Intermixing at Au-In interfaces as studied by photoelectron spectroscopy

H.-G. Boyen, G. Indlekofer,* G. Gantner, H. Stupp, A. Cossy-Favre, and P. Oelhafen
Institut für Physik, Universität Basel, Klingelbergstr. 82, CH-4056 Basel, Switzerland

(Received 9 January 1995)

Interface reactions were observed by means of synchrotron-radiation-induced photoemission during the preparation of Au-In bilayers under UHV conditions at 77 K. These reactions lead to thin amorphous layers with tunable Au content, spanning the same range of compositions as found for vapor-quenched amorphous $\text{Au}_x\text{In}_{100-x}$ alloys. Most importantly, a significant decrease in the electronic density of states towards the Fermi level is observed in the intermixed phase, giving evidence for a strong mutual influence between the conduction electrons and the ionic structure during layer growth.

Since the discovery of solid-state amorphization (SSA) by thermally activated interdiffusion between crystalline Au and La layers as reported by Schwarz and Johnson,¹ considerable experimental and theoretical efforts have been devoted to trying to elucidate the basic principles of this type of amorphization which, obviously, has strong impact on both applied research (e.g., metal-semiconductor systems²) and fundamental studies. For binary systems, a large negative heat of mixing combined with an anomalous high diffusion coefficient of one element within the other is required for a thermally activated amorphization to occur at temperatures of typically some hundred °C.^{3,4} However, the room-temperature preparation of Ni-Zr, Ni-Ti,⁵ and Pt-Al (Ref. 6) multilayers, systems which all show thermally activated SSA, revealed the existence of thin amorphous interface phases even in the as-prepared state without any further heat treatment. In addition, the fabrication of layered structures in the Au-In system has been reported by Seyffert, Siber, and Ziemann^{7,8} to yield intermixed amorphous phases even at cryogenic temperatures. In contrast to the above-mentioned examples, this system was found to exhibit a significantly different behavior because SSA could not be obtained by long-range interdiffusion of thick multilayers. Therefore, based on multiple interface reactions at low temperature, an alternative route into the amorphous state has been proposed.⁷ Recently, these reactions have also been observed at Pd-In, Au-Al, and Au-Sb interfaces,⁹⁻¹² suggesting that amorphization at interfaces should be considered as a rather general phenomenon. In this paper we report about a synchrotron radiation photoemission study performed on Au-In bilayers at low temperature (77 K). The emphasis is put on the characterization of these interface reactions through a precise picture of the electronic structure of the different phases which form during the step-by-step deposition of Au (1–13 ML) onto a polycrystalline In film (thickness 20 nm), and vice versa. These results are compared with photoemission spectra obtained from quench-condensed amorphous $\text{Au}_x\text{In}_{100-x}$ alloys and the pure components.

The photoemission experiments were performed at the synchrotron radiation facility SUPER-ACO at LURE (France), taking advantage of the Swiss-French undulator beam line equipped with a plane grating monochromator.

Using two electron-beam evaporators, the bilayers as well as the amorphous films were prepared *in situ* by vapor condensation onto glass substrates (roughness: 1 nm) held at 77 K. The evaporator sources were adjusted to give growth rates of about 0.01 ML/s controlled by means of a quartz-crystal monitor. During condensation, the pressure was 5×10^{-11} mbar, a necessary condition for preparing contamination-free samples. All valence-band spectra were recorded with a VSW 150-mm hemispherical analyzer using a combined energy resolution (electrons and photons) between 130 and 230 meV (full width at half maximum).

Figure 1 shows a series of angle-integrated valence-band spectra taken at 65-eV incident photon energy after the sequential evaporation of Au onto a freshly prepared polycrystalline In film. According to density-of-states (DOS) calculations,¹³ the valence-band structure of pure

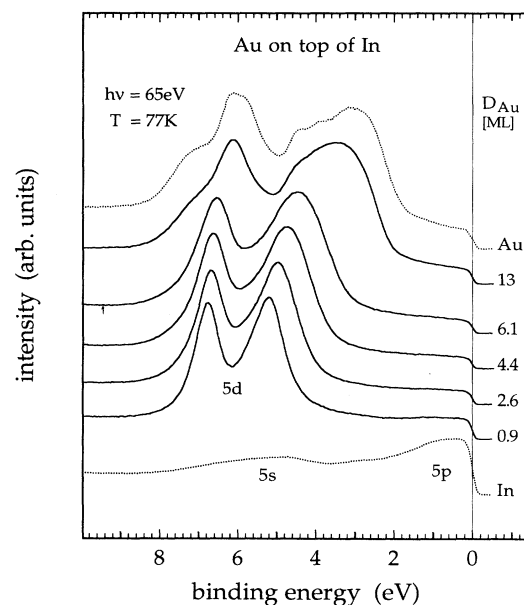


FIG. 1. Valence-band spectra of the Au-In overlayer system for Au coverages up to 13 ML (solid lines). The binding energy is referred to the Fermi level E_F .

In (lowest curve) can be understood as consisting of two subbands, In $5s$ and In $5p$, centered at binding energies of about 5 and 0.7 eV, respectively. After the deposition of 0.9 ML of Au, the electron distribution curve is dominated by two nearly symmetric peaks, corresponding to the Au $5d_{3/2}$ and Au $5d_{5/2}$ bands, respectively. By increasing the amount of adsorbed Au atoms, systematic trends in the development of the curve shape can be recognized: while the Au $5d_{3/2}$ band moves slightly to lower binding energies for Au coverages up to 6.1 ML, a significantly larger shift can be observed for the Au $5d_{5/2}$ band, reflecting a continuous increase in the total bandwidth of Au-derived d states. After depositing 13 ML of Au the band shape drastically changes: now the results are close to those obtained from a 10-nm-thick Au film which is assumed to represent the bulk properties of polycrystalline Au. Hence the adsorption of 13 ML of Au onto polycrystalline In reflects the initial growth of pure (polycrystalline) Au. This is in contrast to the behavior for coverages ≤ 6.1 ML where, according to resistance measurements on Au-In bilayers,⁸ an intermixed amorphous alloy will be expected.

In order to characterize the growth mechanism during the first stage of interface formation in more detail, vapor-quenched $\text{Au}_x\text{In}_{100-x}$ films have also been studied. At cryogenic temperatures, these films are well known to exhibit an amorphous structure for Au concentrations between 20 and 60 at. %.¹⁴ In Fig. 2 a series of valence-band spectra taken on amorphous $\text{Au}_x\text{In}_{100-x}$ alloys are presented (solid lines) together with data measured for the pure components (dotted lines). By analyzing the evolution of the band shape as a function of composition, similar tendencies as in Fig. 1 can be recognized. Whereas the Au $5d_{3/2}$ band position remains nearly constant over the whole range of compositions, a significant

shift toward lower binding energies can be detected for the Au $5d_{5/2}$ band indicating, as in Fig. 1, the continuous increase in the total bandwidth of Au-derived d states. Simultaneously, nearly symmetric peaks can be observed for the emission from the Au $5d$ band, comparable in shape to the results shown in Fig. 1 for Au coverages ≤ 6.1 ML. The striking similarity between the electronic structure of amorphous $\text{Au}_x\text{In}_{100-x}$ alloys and of the interface layer provides the evidence that Au atoms deposited at 77 K on top of polycrystalline In will be strongly chemisorbed, and will result in an intermixed alloy with *disordered* structure for Au coverages up to about 6 ML (corresponding to 1.5 nm).

More details about the growth of the amorphous layer can be extracted from the observed shifts. In Fig. 3(a) the binding energy values of the Au $5d_{5/2}$ band maximum are given as a function of the Au overlayer thickness D_{Au} [evaluated from Fig. 1, left scale in Fig. 3(a)] and the Au concentration X [evaluated from Fig. 2, right scale in Fig. 3(a)]. Solid lines have been added as a guide to the eyes. Obviously, the chemisorption of Au atoms onto In leads to a monotonic decrease of the binding energy of the Au $5d_{5/2}$ band, thereby indicating a steadily rising Au content of the intermixed phase during film growth. This is in contrast to previous suggestions, where a single composition has been proposed [Au:In=1:2 (Ref. 8)]. By relating the binding-energy shifts of both systems, a rough estimate of the effective Au concentration X_{eff} of the intermixed layer can be obtained. This leads directly to an estimate of the In contribution $D_{\text{eff,In}}$ to the reacted layer by combining X_{eff} with the corresponding D_{Au} values. The results are presented in Fig. 3(b), showing that X_{eff} (right scale), for an overlayer thickness of about 6 ML reaches a value of approximately 60 at. %, which coincides with the maximum Au content of the homogeneous amorphous phase [$X \approx 60$ at. % (Ref. 14)]. Simultaneously, $D_{\text{eff,In}}$ (left scale) does not vary with D_{Au} within the estimated error bars, implying a nearly constant In contribution to the intermixed phase of approximately 4–5 ML.

Based on resistance measurements, interfacial reactions at low temperature have also been reported in the case of In atoms deposited on top of polycrystalline Au.⁸ However, the amorphization processes have been ascertained to saturate at overlayer thicknesses of 1.1 nm (corresponding to a nominal thickness of 3.7 ML), i.e., at a significant lower value as compared to the chemisorption of Au on top of In. This different behavior should also be visible in a photoemission experiment, allowing a further critical test of the idea that an amorphous phase will form at interfaces even at low temperature. Figure 4 shows the valence-band spectra of the corresponding In-Au interface, prepared by sequential evaporation of In on top of polycrystalline Au. Again the electronic structure of the obtained interface layer clearly indicates a strong reaction of the In atoms with the Au substrate film. During the depositing of In at 77 K the Au $5d_{5/2}$ band undergoes a significant shift at higher binding energies, reaching a stable position (≈ 5.1 – 5.2 eV) at an In coverage $D_{\text{In}} \approx 4$ ML. The formation of an amorphous intermixed layer, which can be concluded from the results reported

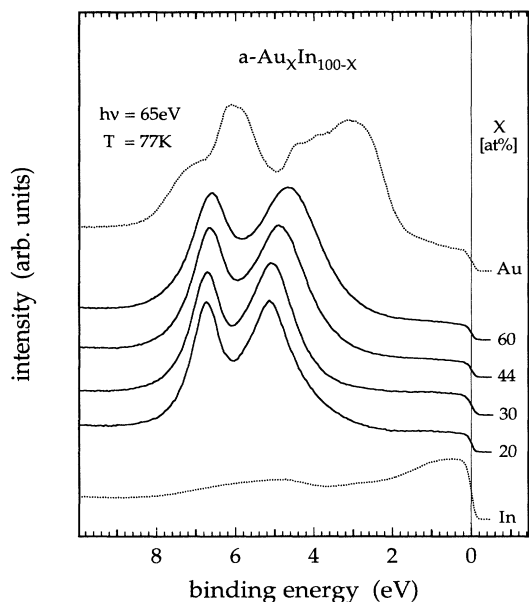


FIG. 2. Valence-band spectra of vapor-quenched amorphous $\text{Au}_x\text{In}_{100-x}$ alloys (solid lines).

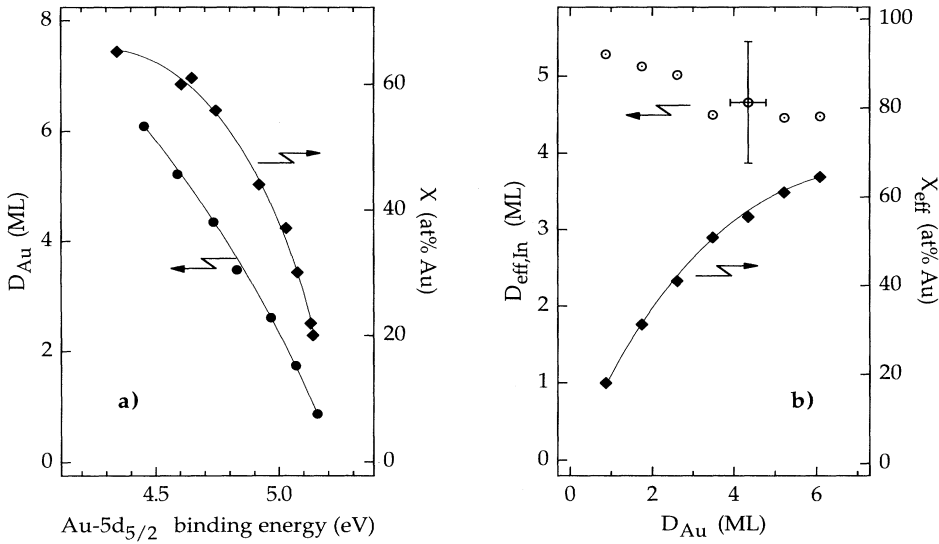


FIG. 3. Analysis of relevant parameters during interface formation: (a) Position of the Au $5d_{5/2}$ valence-band maximum plotted as function of the Au overlayer thickness D_{Au} (left axis), and the Au concentration of the vapor-quenched amorphous alloys X (right axis), respectively. Solid lines have been added as guide to the eye. (b) Estimated values for the average Au concentration of the intermixed phase, X_{eff} (right axis), and the effective thickness of the In contribution to the reacted phase $D_{eff,In}$ (left axis) vs. Au overlayer thickness D_{Au} .

so far, is now accompanied by the presence of a certain amount of unreacted polycrystalline Au as indicated by the existence of a shoulder at binding energies of ≈ 3 eV. Despite the detection of unreacted Au, the growth of the amorphous interlayer can be discussed as a continuous decrease of the effective Au concentration, reaching its minimum value of ≈ 20 at. % [see Fig. 3(a), right scale] for an In coverage of about 4 ML, which agrees fairly well with the number quoted in Ref. 8. For higher coverages the growth of an additional third component, polycrystalline In, becomes evident from the development of the band shape near the Fermi level. Again the thickness of the intermixed layer is found to be limited due to an effective Au content which reaches the boundary condition of amorphous Au_xIn_{100-x} alloys [20 at. %

$\leq X \leq 60$ at. % (Ref. 14)].

Based on the observed strong similarities between the interlayer results and the data of quench-condensed amorphous films, one might expect that other electronic effects should also be relevant for the intermixed phase, which are known to be of basic importance for the forming ability of this type of alloy (noble metal/polyvalent element). This class of alloys, which has been identified by Häussler as a Hume-Rothery phase with an amorphous structure,¹⁴ exhibits remarkable interrelations between electronic and ionic structures (for a review, see Ref. 15). Briefly, the ionic structure is observed to depend strongly on the average number of conduction electrons per atom (which can be modified by alloying), leading to strong medium-range order in the amorphous phase due to atomic positions which correspond to Friedel minima in the effective interatomic potential. This, on the other hand, has been demonstrated¹⁶ to give rise to a pseudogap or structure-induced minimum in the density of states (MDOS) of conduction electrons near the Fermi level, lowering the total energy of the electronic system as compared to a free-electron model, thereby stabilizing the amorphous phase as originally proposed by Nagel and Tauc.¹⁷

Assuming that this description is also relevant for the amorphous interlayer, a pseudogap is to be expected at the Fermi level as long as amorphization processes are observed. Indeed, such a behavior can be seen in Fig. 5, where the low-binding-energy range has been plotted on an enlarged scale for the homogeneously intermixed layers (Au on top of In). Obviously, a significant decrease of the DOS curves toward the Fermi level is detected (shaded area), which is more pronounced for higher Au coverages. This result nicely correlates with the observations on various amorphous Hume-Rothery alloys, revealing the most pronounced MDOS in the case of the highest noble-metal content of the disordered alloy.⁵ It can be assigned to an optimum matching between the isotropic pseudo-Brillouin-zone and the isotropic Fermi sphere occurring at an average value of 1.8 conduction electrons

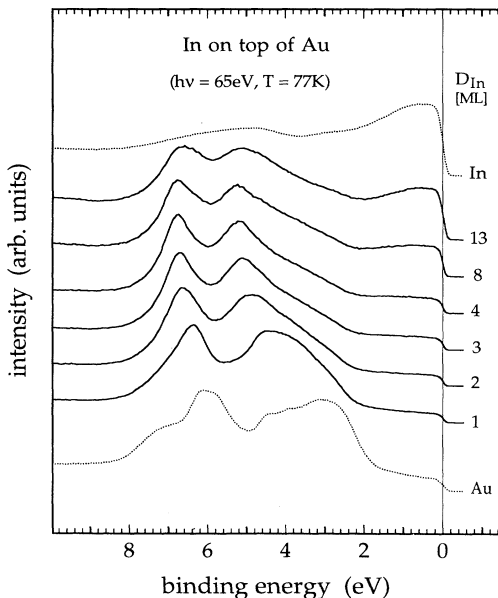


FIG. 4. Valence-band spectra of the In-Au overlayer system for In coverages up to 13 ML (solid lines).

per atom.¹⁵ Complementary to the discussion based on effective interatomic potentials, this number has recently been calculated¹⁸ to yield the most constructive interference of electrons scattered by the atomic structure of the disordered phase.

These findings reflect unambiguously the importance of electronically induced effects on the atomic structure of the intermixed phase during the interlayer growth. Since long-range interdiffusion always results in crystalline Au-In phases,^{7,8} a different mechanism must be responsible for the formation of the amorphous layers. Hence the existence of a pseudogap in the conduction-electron density of states at the Fermi level can be taken as a starting point for the discussion of the thermodynamical driving forces necessary to explain the formation of an intermixed phase with disordered structure.

In conclusion, synchrotron-radiation-induced photoemission has been applied to study the effects of intermixing at Au/In interfaces at 77 K. Au/In—as well as In/Au—bilayers were analyzed with respect to data taken on quench-condensed amorphous $\text{Au}_x\text{In}_{100-x}$ alloys. Evidence has been found that for coverage ≤ 6 ML, the deposition of Au onto polycrystalline In leads to the formation of an intermixed amorphous layer with Au concentrations as high as $X \approx 60$ at. %, corresponding to the maximum Au content of vapor-quenched amorphous films.¹⁴ For In atoms deposited on top of polycrystalline Au, amorphization reactions are observed to occur for coverages up to 4 ML, leading to a minimum Au concentration of the intermixed phase of $X \approx 20$ at. %. In this case contributions of polycrystalline Au to the valence-band spectra are detected. For the homogeneously reacted amorphous interlayer, a significant decrease in the electronic density of states toward the Fermi level E_F is observed, indicative of the strong influence of the conduction electrons on the ionic structure of the intermixed

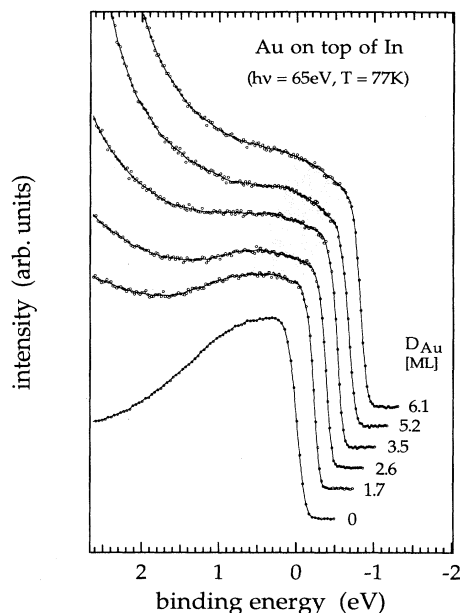


FIG. 5. Low-binding-energy range of the spectra shown in Fig. 1, reflecting a decrease of the density-of-state curves towards the Fermi energy E_F . All data have been corrected for secondary-electron contributions as well as for the transmission function of the energy analyzer.

phase, and vice versa. This interrelation can be used to discuss the growth of the amorphous interlayer in terms of simple band-structure arguments.

We thank Professor P. Häussler and Professor P. Ziemann for valuable discussions, and Dr. A. Mansour for carefully reading the manuscript. This work has been supported by the Swiss National Science Foundation.

*Present address: LURE, Centre Universitaire de Paris-Sud, Bâtiment 209D, F-91405 Orsay cedex, France.

¹R. B. Schwarz and W. L. Johnson, Phys. Rev. Lett. **51**, 415 (1983).

²L. J. Chen, W. Lur, and J. Y. Cheng, Thin Solid Films **191**, 221 (1989).

³W. L. Johnson, Prog. Mater. Sci. **30**, 81 (1986).

⁴K. Samwer, Phys. Rep. **161**, 1 (1988).

⁵B. M. Clemens, Phys. Rev. B **33**, 7615 (1986).

⁶B. Blanpain, L. H. Allen, J.-M. Legresy, and J. W. Mayer, Phys. Rev. B **39**, 13 067 (1989).

⁷M. Seyffert, A. Siber, and P. Ziemann, Phys. Rev. Lett. **67**, 3792 (1991).

⁸M. Seyffert, A. Siber, and P. Ziemann, Thin Solid Films **208**, 197 (1992).

⁹A. Siber, J. Marien, T. Koch, and P. Ziemann, Appl. Phys. A **57**, 267 (1993).

¹⁰R. Fink, T. Koch, G. Krausch, J. Marien, A. Plewnia, B.-U. Runge, G. Schatz, A. Siber, and P. Ziemann, Phys. Rev. B **47**, 10 048 (1993).

¹¹T. Koch, A. Siber, J. Marien, and P. Ziemann, Phys. Rev. B **49**, 1996 (1994).

¹²H.-G. Boyen, A. Cossy-Favre, P. Oelhafen, A. Siber, P. Ziemann, C. Lauinger, T. Moser, P. Häussler, and F. Baumann, Phys. Rev. B **51**, 1791 (1995).

¹³D. A. Papaconstantopoulos, *Handbook of the Band Structure of Elemental Solids* (Plenum, New York, 1986).

¹⁴P. Häussler, Z. Phys. B **53**, 15 (1983).

¹⁵P. Häussler, Phys. Rep. **222**, 65 (1992).

¹⁶P. Häussler, F. Baumann, J. Krieg, G. Indlekofer, P. Oelhafen, and H.-J. Günthrod, Phys. Rev. Lett. **57**, 714 (1983).

¹⁷S. R. Nagel and J. Tauc, Phys. Rev. Lett. **35**, 380 (1975).

¹⁸H. Solbrig and R. Arnold (unpublished).

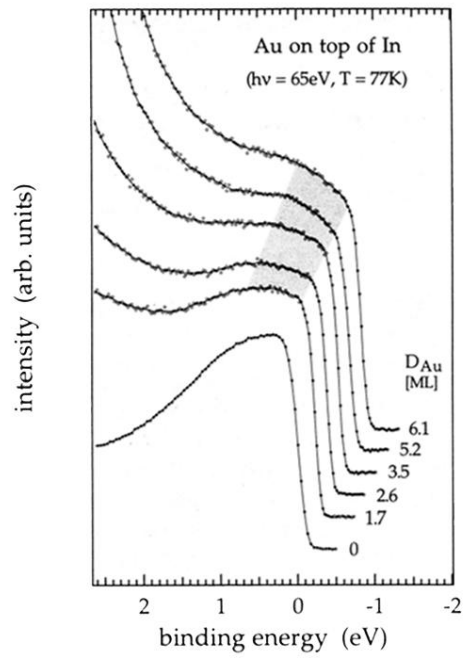


FIG. 5. Low-binding-energy range of the spectra shown in Fig. 1, reflecting a decrease of the density-of-state curves towards the Fermi energy E_F . All data have been corrected for secondary-electron contributions as well as for the transmission function of the energy analyzer.